CHAPTER IV

RESULTS AND DISCUSSION

4.1 Degree of organoclay dispersion in iPP composites

A degree of layered silicate dispersion in polymer matrix strongly affects the mechanical properties of polymer/clay nanocomposites [16-17]. Especially, polymer/clay nanocomposites, which clay is exfoliated throughout the polymer matrix, are desirable for improving various properties due to a high aspect ratio of clay and a large interfacial area between polymer and layered silicates. X-ray diffraction (XRD) is the characterization technique commond, used to determine a d-spacing of layered silicates or identify nanocomposite structures. D-spacing and diffraction peak of pristine clay, organoclay and all composites were summarized in Table A.1 (Appendix A).

XRD patterns of pristine clay, organoclay are illustrated in Figure 4.1. It can be seen that the peak showing a d-spacing of pristine clay was at $2\theta = 7.01^\circ$ corresponding to a d-spacing of 1.26 nm. Organoclay exhibited an intense peak at $2\theta = 4.61^\circ$ corresponding to a d-spacing of 1.92 nm. The shift of diffraction peak to lower angle indicated the increased of d-spacing.

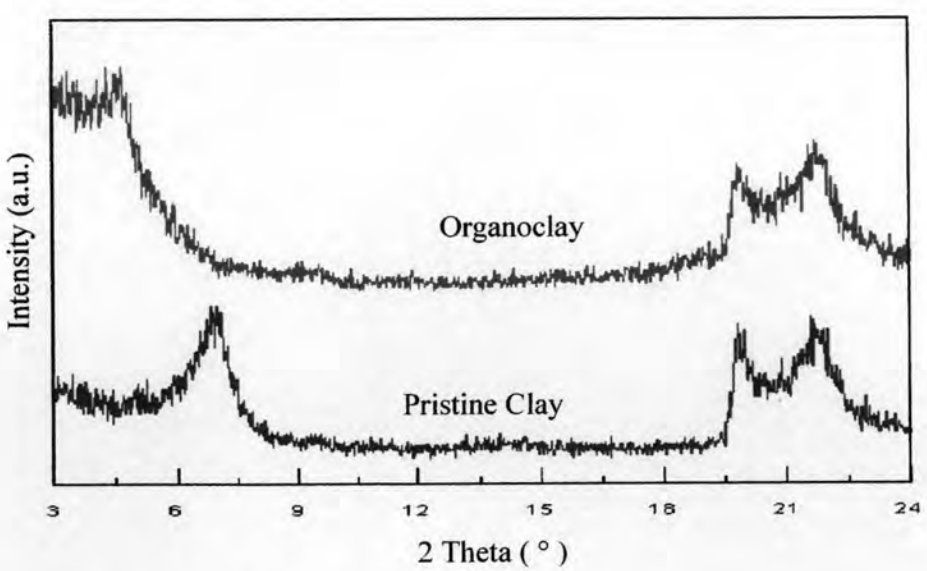

Figure 4.1 XRD patterns of clay and organoclay.

The organoclay was melted mixing with iPP and extruded through a twin screw extruder attached to injection mold at 3 wt% of organoclay loading. From Figure 4.2, the XRD signals of iPP/organoclay nanocomposite appeared at $2\theta = 4.66^{\circ}$ and 6.84° which corresponded to a d-spacing of 1.89 and 1.29 nm, respectively. The distance between layered silicates decreased when organoclay was added to iPP matrix. The decrease in a d-spacing of layered silicates in iPP/organoclay nanocomposite could be resulted from the rearrangement of surfactant between layered silicates while mixing iPP with organoclay.

Furthermore, the diffraction intensity of iPP/organoclay nanocomposite was gradually increased when organoclay was added. The increase in diffraction intensity of XRD peak led to a high order of layered silicates that dispersed into iPP matrix. From Figure 4.2, it can be seen that the orientation of layered silicates of iPP/organoclay nanocomposite was more orderly than that of iPP/GF composite. However, XRD diffraction patterns of neat iPP, iPP/GF composite and iPP/organoclay nanocomposite all exhibited a peak at $2\theta = 16.6^{\circ}$. This peak is associated with β-crystalline formation (hexagonal) of iPP matrix [32]. This implies that the crystalline domain of iPP matrix can still be formed in the presence of fillers (both GF and organoclay).

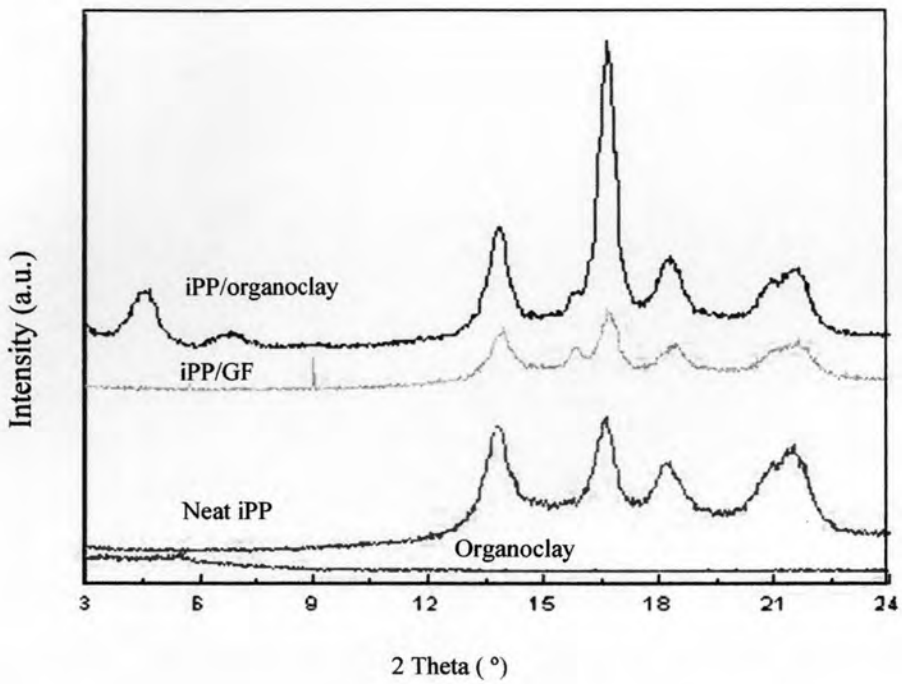

Figure 4.2 XRD patterns of organoclay, neat iPP, iPP/GF composite and iPP/organoclay nanocomposite.

From Figure 4.2, it can also be seen that the orientation of layered silicate in iPP/organoclay nanocomposite was more orderly than the original organoclay. The fact that the peak $2\theta = 16.6°$ of iPP/organoclay nanocomposite was sharper than that of the neat iPP suggested that the crystallinity of iPP be increased upon the composite formation with organoclay. It is believed that layered silicates can serve as a nucleating agent for iPP crystallization. Obviously, this was not the case for the iPP/GF composite. The area under diffraction peaks of iPP/GF composite was apparently smaller as compared with those of both neat iPP and iPP/organoclay nanocomposite. The area under XRD diffraction peaks of neat iPP, iPP/GF composite and iPP/organoclay nanocomposite are illustrated in Table 4.1.

Table 4.1 Degree of crystallinity of iPP composites calculated from the area of diffraction peak of XRD.

Sample	Peak Area	Degree of Crystallinity (%)
neat iPP	5,237.7	40.05
iPP/GF composite	2,960.2	40.14
iPP/organoclay with compatibilizer	4,796.2	47.87
iPP/GF : iPP/organoclay 90 : 10	979.7	50.23
iPP/GF : iPP/organoclay 70 : 30	1,369.3	54.85
iPP/GF : iPP/organoclay 50 : 50	1,179.9	57.65

As shown in Figure 4.3 and Figure 4.4, XRD pattern of all blended composites exhibited peaks at $2\theta = 4.66^{\circ}$ and 6.84° (corresponding to a d-spacing of 1.89 and 1.29 nm, respectively) which are characteristic peaks of layered silicate in the iPP/organoclay nanocomposite. As anticipated, the peak intensity of XRD pattern belonging to the layered silicate in organoclay increased as a function of the iPP/organoclay content in the blended composite. The peak areas of all blended composites are summarized in Table 4.1. The increase in area under the diffraction peak indicated that the addition of organoclay enhanced the growth of crystalline part of iPP matrix. Furthermore, the fact that the XRD patterns and d-spacing of the layered silicates of the blended composites were not different from that of the starting iPP/organoclay nanocomposite implied that the melt mixing process used for making the blended composites in this experiment and content of GF did not affect the distribution of layered silicates of the organoclay. In other words, the melt mixing process did not disturb the role of layered silicates serving as a nucleating–agent for iPP crystallization. As a consequence the degree of iPP crystallinity increased as the content of organoclay increased.

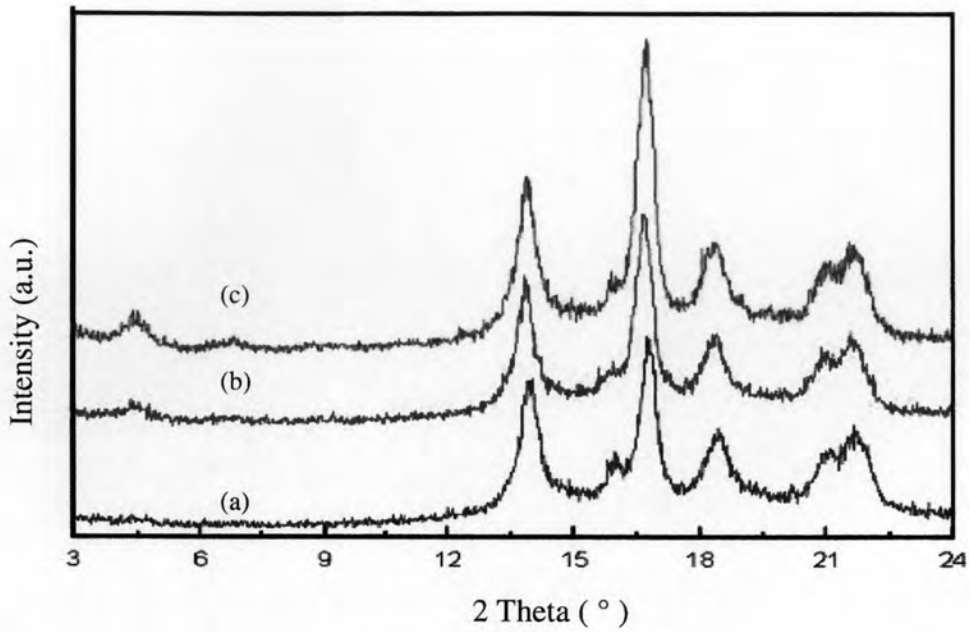

Figure 4.3 XRD patterns of blended nanocomposite at various ratios of iPP/GF composite and iPP/organoclay nanocomposite: (a) 90:10, (b) 70:30, and (c) 50:50.

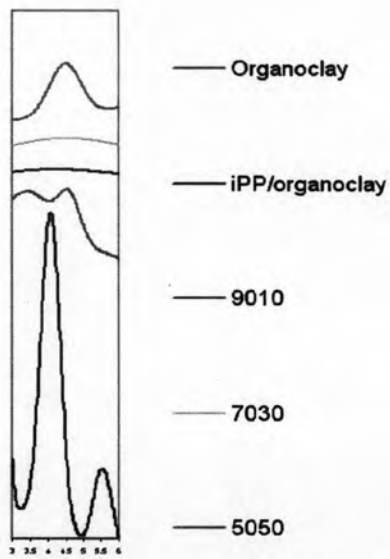

Figure 4.4 XRD patterns of blended nanocomposite at $2\theta = 3^{\circ}$-6°.

SEM micrographs of all blended composites shown in Figure 4.5 only exhibited the presence of glass fibers not the organoclay. It can be seen from TEM micrographs shown in Figure 4.6 that the organoclay in all blended composites was in the form of stacks of layered silicates that presumably intercalated with iPP matrix.

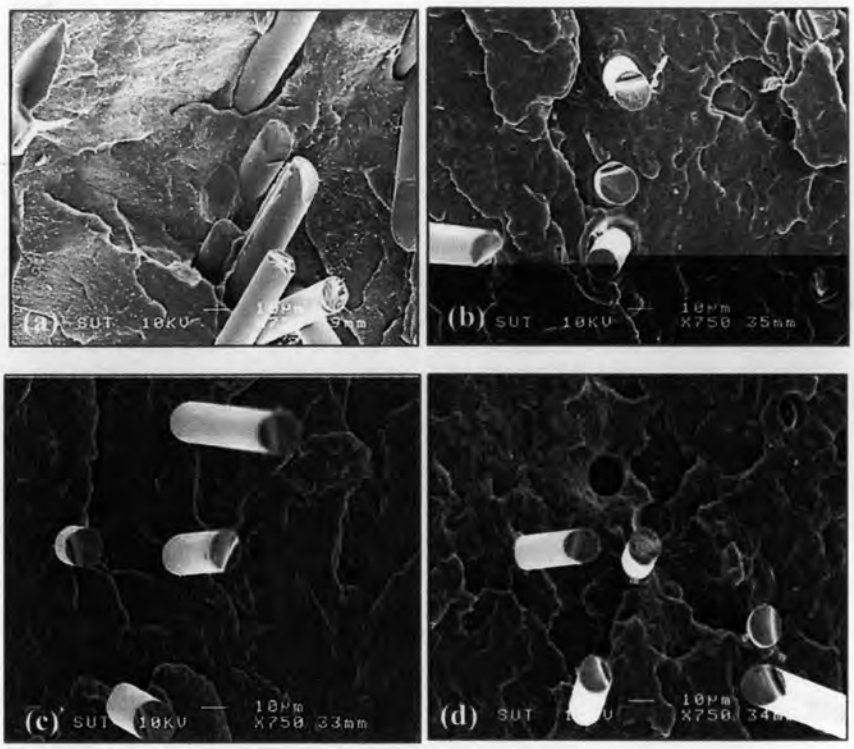

Figure 4.5 SEM micrographs of blended composites at various ratios of iPP/GF composite and iPP/organoclay nanocomposite: (a)100:0, (b) 90:10, (c) 70:30, and (d) 50:50.

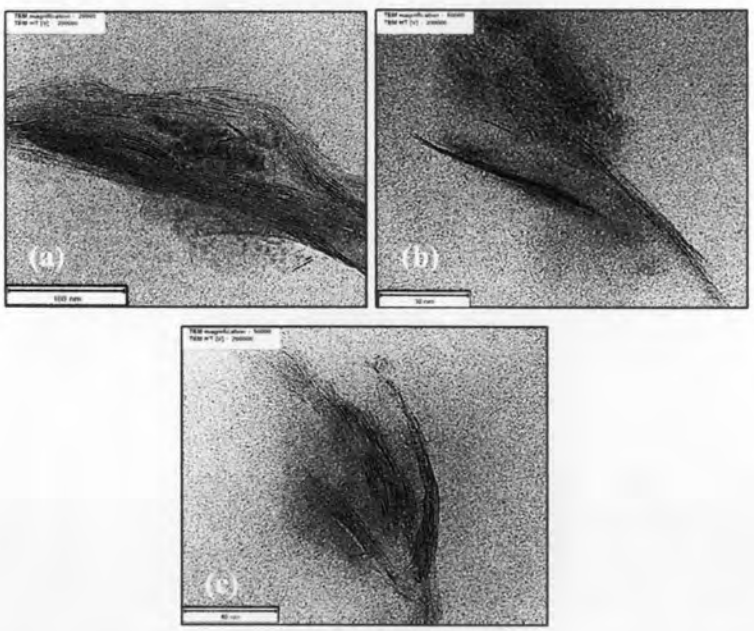

Figure 4.6 TEM micrographs of blended composites at various ratios of iPP/GF composite and iPP/organoclay nanocomposite: (a)100:0, (b) 90:10, and (c) 50:50.

4.2 Thermal properties of iPP composites.

Thermal properties of neat iPP and iPP composites were determined by differential scanning calorimetry, DSC. The melting (T_m) and crystallization temperature (T_c) of iPP composites are summarized in Table 4.2. DSC heating curves at the rate of 10°C/min of neat iPP and iPP composites are shown in Figure 4.6.

Table 4.2 Melting (T_m) and crystallization temperature (T_c) of composites

Sample	Melting temperature, T_m (°C)	Crystallization temperature, T_c (°C)
neat iPP	162.9[1]	111.2
iPP/GF	158.0[2] 164.0[1]	114.6
iPP/organoclay with compatibilizer	151.5[2] 164.6[1]	116.3
iPP/GF : iPP/organoclay 90 : 10	158.5[2] 164.0[1]	116.8
iPP/GF : iPP/organoclay 70 : 30	158.5[2] 163.4[1]	118.0
iPP/GF : iPP/organoclay 50 : 50	158.5[2] 163.4[1]	116.3

[1]is donated as α-crystalline phase of iPP matrix [32].

[2]is donated as β-crystalline phase of iPP matrix [32].

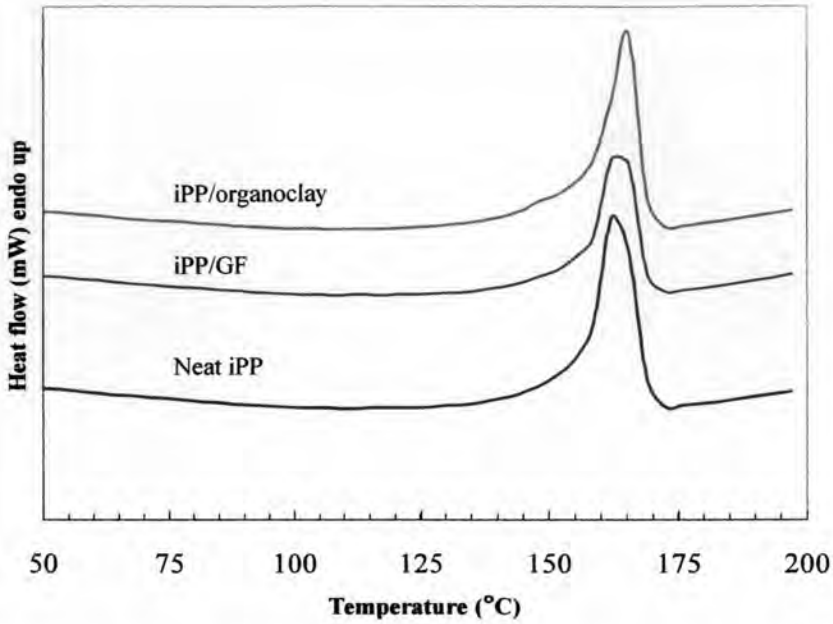

Figure 4.7 DSC heating profiles of neat iPP and iPP composites at a heating rate of 10°C/min.

Neat iPP showed only one melting peak at 162.9°C, corresponding to the α-crystalline phase of iPP, which was different from XRD results (only β-crystalline form was observed) [5]. IPP was heated from room temperature to 200°C; therefore, polymer chains can be rearranged and formed more stable α-crystalline phase during heating. After mixing iPP with organoclay, the nanocomposite exhibited two melting peaks at 151.5 and 164.6°C, which were β and α-crystalline phase of iPP respectively. However, α-crystalline phase of iPP was still dominant for all nanocomposites. This result indicated that the addition of layered silicates into iPP matrix enhanced the formation of β-crystalline phase of iPP.

After heating to 200°C, nanocomposites were then cooled at 10°C/min in which the cooling profiles were shown in Figure 4.8. An exothermic crystallization peak of the neat iPP exhibited a crystallization temperature at 111.2°C. Interestingly, when organoclay was added into iPP matrix, crystallization temperature was shifted to higher temperature than the neat iPP about 5.1°C. However, crystallization temperature of iPP/organoclay nanocomposite shifted to the higher temperature than iPP/GF composite. This indicated that the addition of layered silicates into iPP matrix enhanced the rate of crystallization, which could be observed from the increasing crystallization temperature. In the other words, layered silicates served as an additional nucleating agent [32]. Moreover, they can also enhance the rate of iPP crystallization better than the glass fiber.

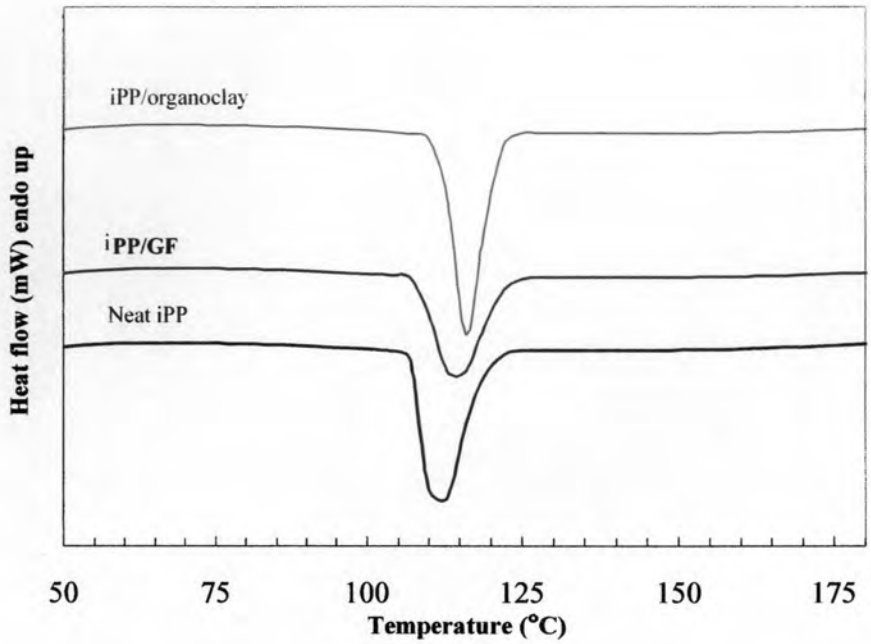

Figure 4.8 DSC cooling profiles of neat iPP and iPP composites at a cooling rate of 10°C/min.

Heating profiles of the blended composites are shown in Figure 4.9. The melting temperature slightly decreased with increasing iPP/organoclay loading. The blended composites exhibited two melting peaks at 158.5 and 163.4°C, which corresponded to the β and α-crystalline phase of iPP respectively, for all iPP/organoclay loading. From above results, it should be noted that the addition of iPP/organoclay also enhanced the rate of crystallization as demonstrated by the increasing crystallization temperature with increasing iPP/organoclay loading to 30 wt% (Figure 4.10). However, the lower crystallization temperature was observed at iPP/organoclay loading of 50 wt%.

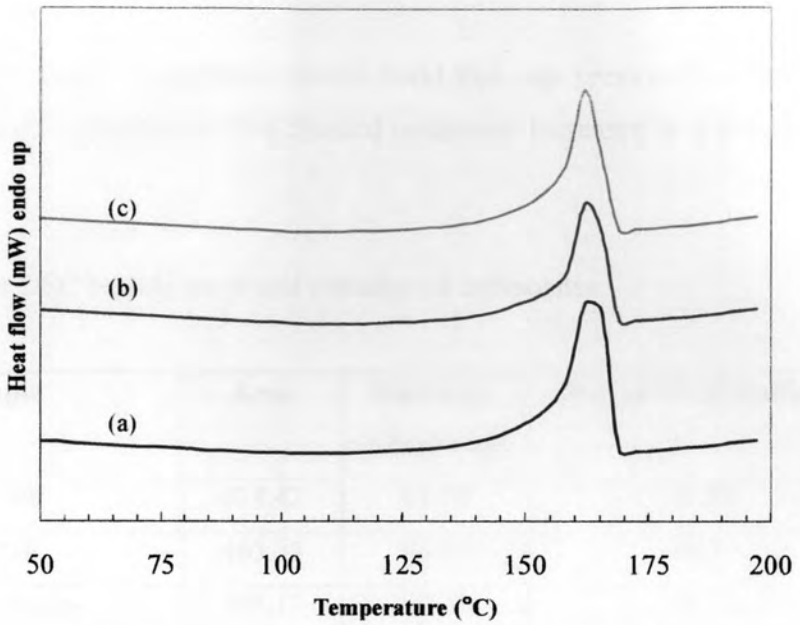

Figure 4.9 DSC heating profiles of blended composite at various ratios of iPP/GF composite and iPP/organoclay nanocomposite: (a) 90:10, (b) 70:30 and (c) 50:50 at a heating rate of 10°C/min.

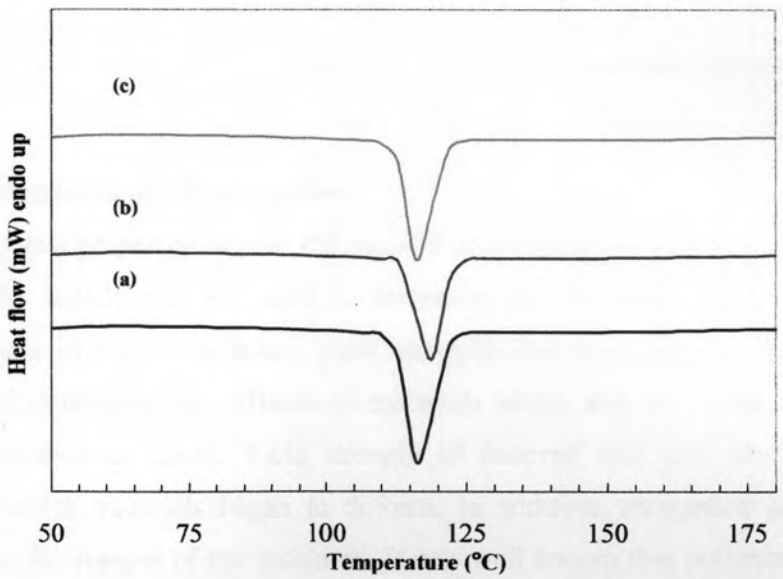

Figure 4.10 DSC cooling profiles of blended composite at various ratios of iPP/GF composite and iPP/organoclay nanocomposite: (a) 90:10, (b) 70:30 and (c) 50:50 at a cooling rate of 10°C/min.

should be also considered because it strongly affected the improvement of mechanical properties. Besides inorganic filler, the crystalline part of polymer also enhances the stiffness of polymer. In general, the stiffness of materials increases with increasing degree of crystallinity.

From Figures 4.11-4.12, tensile modulus of iPP/organoclay with 3 wt% of organoclay and iPP/GF with 10 wt% of GF were higher than that of the neat PP. The tensile modulus of iPP increased by 119.6 and 153% when organoclay and GF were incoporated, respectively. In similar trend, yield strength of iPP/organoclay and iPP/GF increased by 150.4 and 192.9%, respectively in comparison with that of the neat iPP. The increase of tensile modulus and yield strength for both iPP/organoclay nanocomposite and iPP/GF composite may be mainly caused by the addition of inorganic filler (organoclay and fiber glass) that acts as a reinforcement agent into iPP matrix. Elongation at break of the iPP composites as shown in Figure 4.13 decreased by 34.6% when organoclay was added into iPP matrix. While the elongation at break of iPP/GF composite decreased by 65.6%. This indicated that the additional of inorganic material caused the iPP composite to be less ductile or more brittle because this led to higher stiffness.

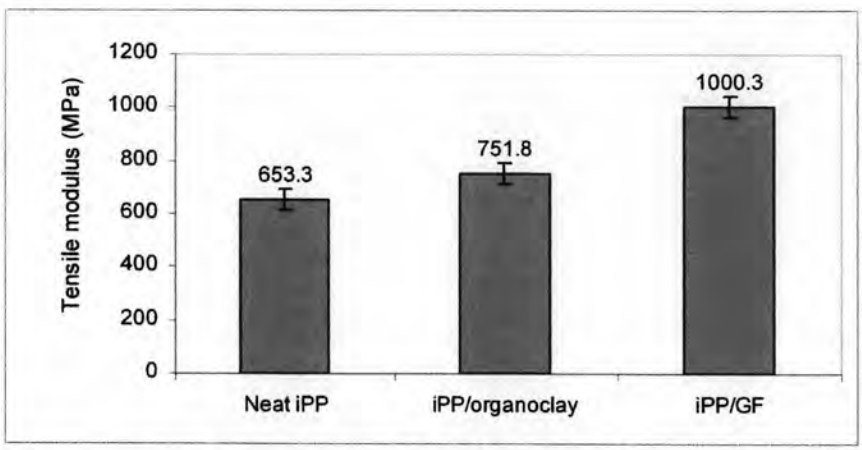

Figure 4.11 Tensile modulus of neat iPP and iPP composites.

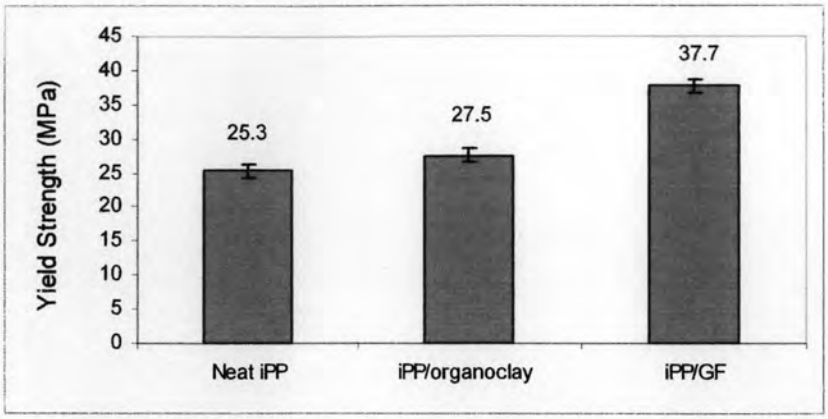

Figure 4.12 Yield strength of neat iPP and iPP composites.

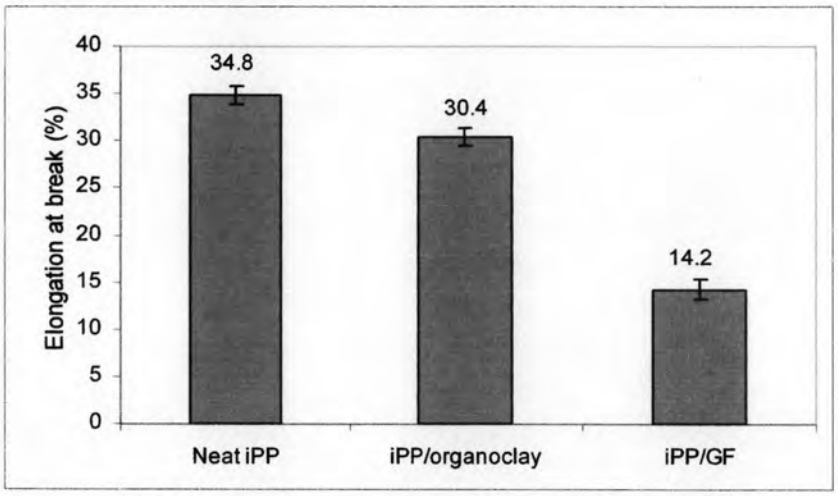

Figure 4.13 Elongation at break of neat iPP and iPP composites.

From Figures 4.11-4.13, it can be seen that iPP/GF composite exhibited higher stiffness than the iPP/organoclay nanocomposite. This could be explained by interfacial interaction between inorganic material and iPP matrix which can be demonstrated by SEM and TEM micrographs shown in Figures 4.5 and 4.6, respectively. It is suspected that iPP/organoclay nanocomposite exhibited higher stiffness than the neat iPP because the organoclay not only acts as a reinforcement agent, but also behaves as a nucleating agent for iPP crystallization. The addition of organoclay helped enhancing the crystallinity of iPP matrix and thus made the composite more stiff.

The same trends were also observed for mechanical properties of the blended composites as shown in Figures 4.14-4.16. In comparison with iPP/GF composite, tensile modulus were 190.1, 184.3 and 175.1% when the iPP/organoclay nanocomposite loading of 10, 30, and 50 wt% were added, respectively. But there was no variation between yield strength of the blended composites having different iPP/organoclay nanocomposite loading.

For elongation at break, the blended composites were increased as a function of iPP/organoclay loading. As compared with the iPP/GF composite, the elongation at break of the blended composite increased by 57.3, 62.6 and 71.4% when iPP/organoclay nanocomposite of 10, 30 and 50 wt% was added, respectively.

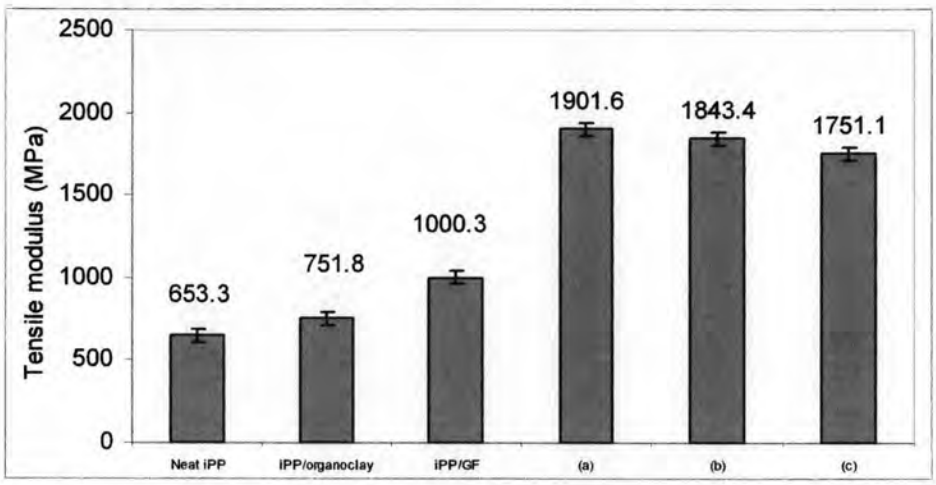

Figure 4.14 Tensile modulus of composite and blended composite at various ratios of iPP/GF composite and iPP/organoclay nanocomposite: (a) 90:10, (b) 70:30, and (c) 50:50.

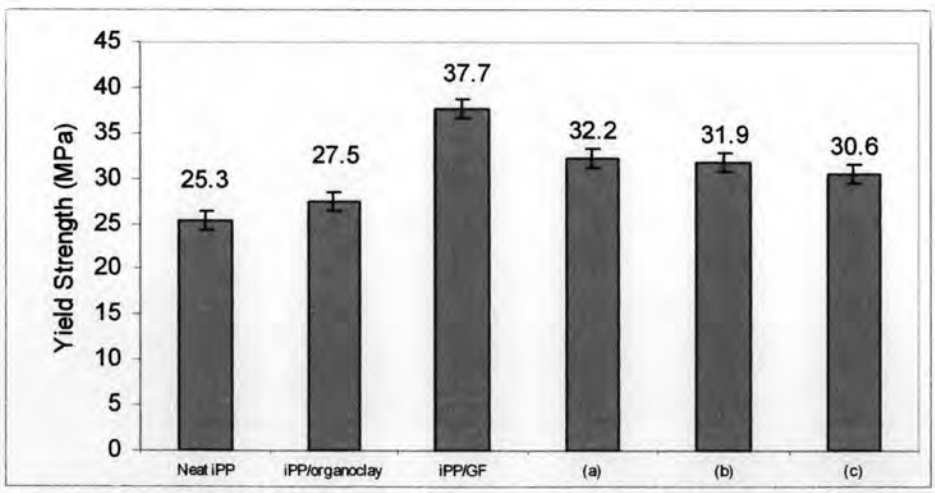

Figure 4.15 Yield strength of composite and blended composite at various ratios of iPP/GF composite and iPP/organoclay nanocomposite: (a) 90:10, (b) 70:30, and (c) 50:50.

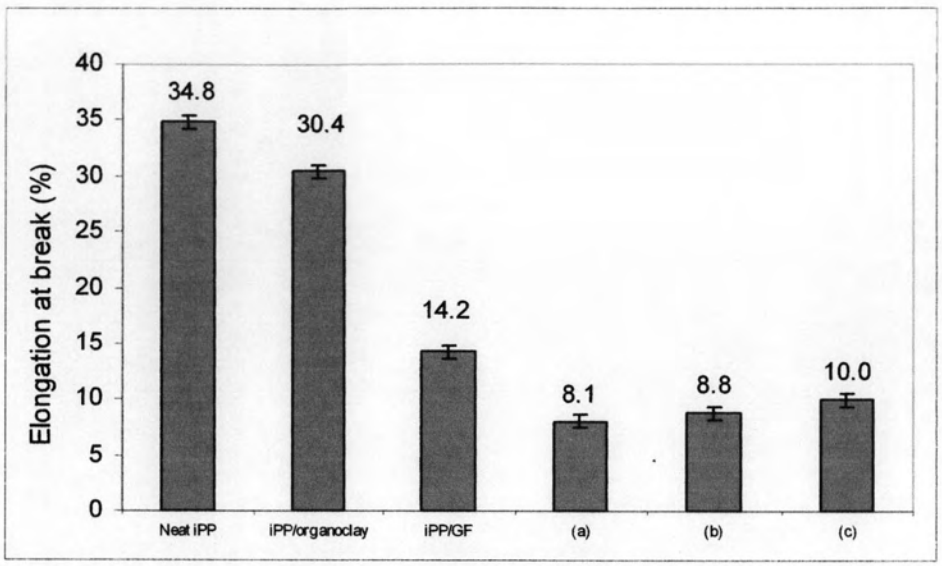

Figure 4.16 Elongation at break of composite and blended composite at various ratios of iPP/GF composite and iPP/organoclay nanocomposite: (a) 90:10, (b) 70:30, and (c) 50:50.